

Supporting Information for

**Low-cost One-Pot Synthesis of Hydrophobic and Hydrophilic
Monodispersed Iron Oxide Nanoparticles**

Sohel Reja,* Manoj Kumar and Sukumaran Vasudevan

^a Department of Inorganic and Physical Chemistry,

Indian Institute of Science, Bangalore-560012, India

*Corresponding Author: sohelreja@iisc.ac.in

Table of contents:

1. Fig. S1: PXRD and ATR-IR spectrum of intermediate iron hydroxide.
2. Fig. S2: ATR-IR spectra of oleic acid coated iron oxide nanoparticles and *in-situ* formed iron oleate complex.
3. Fig. S3: SAED and FFT of spherical nanoparticles
4. Fig. S4: SAED and FFT of spherical nanoparticles with oleyl alcohol
5. Fig. S5: SAED and FFT of cubic nanoparticles
6. Fig. S6: SAED and FFT of phase-transferred spherical and cubic nanoparticles
7. Fig S7: TEM images of nanoparticles from different starting alcohol
8. Fig S8: ATR-IR spectra of oleic acid and NTA-coated iron oxide nanoparticles
9. Fig S9: DLS and zeta potential of the NTA-capped iron oxide nanoparticles
10. Fig S10: TEM image of scaled-up synthesized iron oxide nanoparticles
11. Table S1: Particle size for different reflux times
12. Table S2: Particle size for different starting alcohols

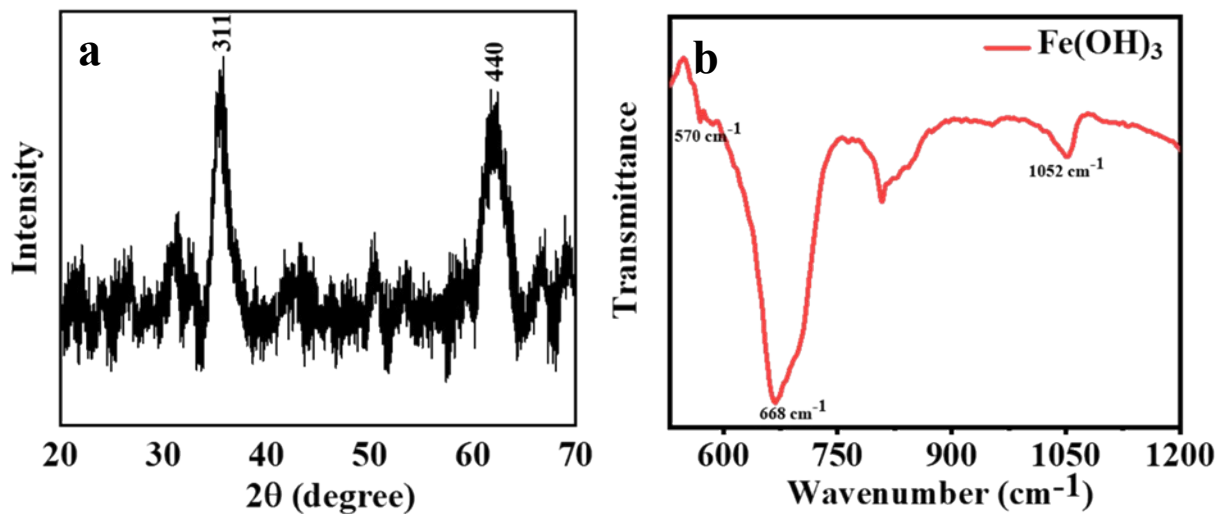


Fig. S1: a) PXRD and b) ATR-IR spectrum of iron hydroxide. The Bragg reflections at $2\theta=35^\circ$ and 62° may be assigned to the (311) and (440) planes of the cubic iron hydroxide phase (JCPDS no. 22-0346)^{1,2}. In the ATR-IR spectra (Fig. S1b), the absorption bands at 570, 668, and 1052 cm^{-1} may be assigned to Fe-O vibrations of iron hydroxide.³⁴.

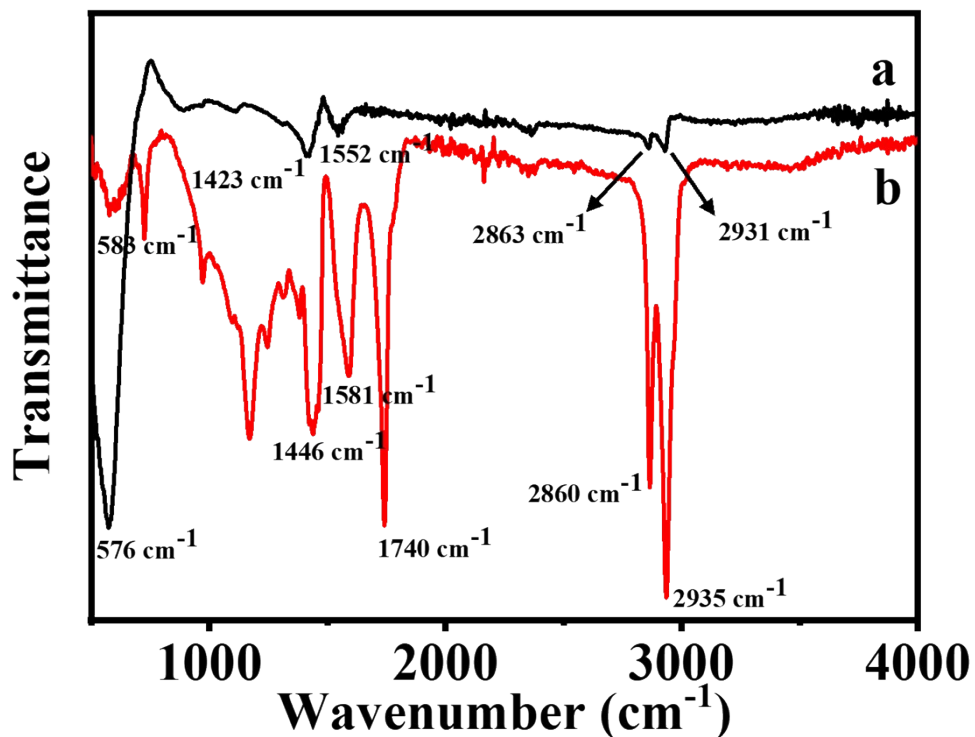


Fig. S2: ATR-IR spectra of the product of *in-situ* prepared iron oleate (b) and oleic acid capped iron oxide nanoparticle (a). The assignment of the peaks is as follows: iron oleate (b): 2935,

2860: sp₃ C-H stretching vibration; 1740: C=O stretching vibration; 1446, 1581: symmetric and asymmetric -COO stretching; 576: Fe-O stretching. Oleic acid-capped iron oxide (a): 2931,2863: sp₃ C-H stretching vibration; 1423, 1552: symmetric and asymmetric -COO stretching; 583: Fe-O stretching⁵.

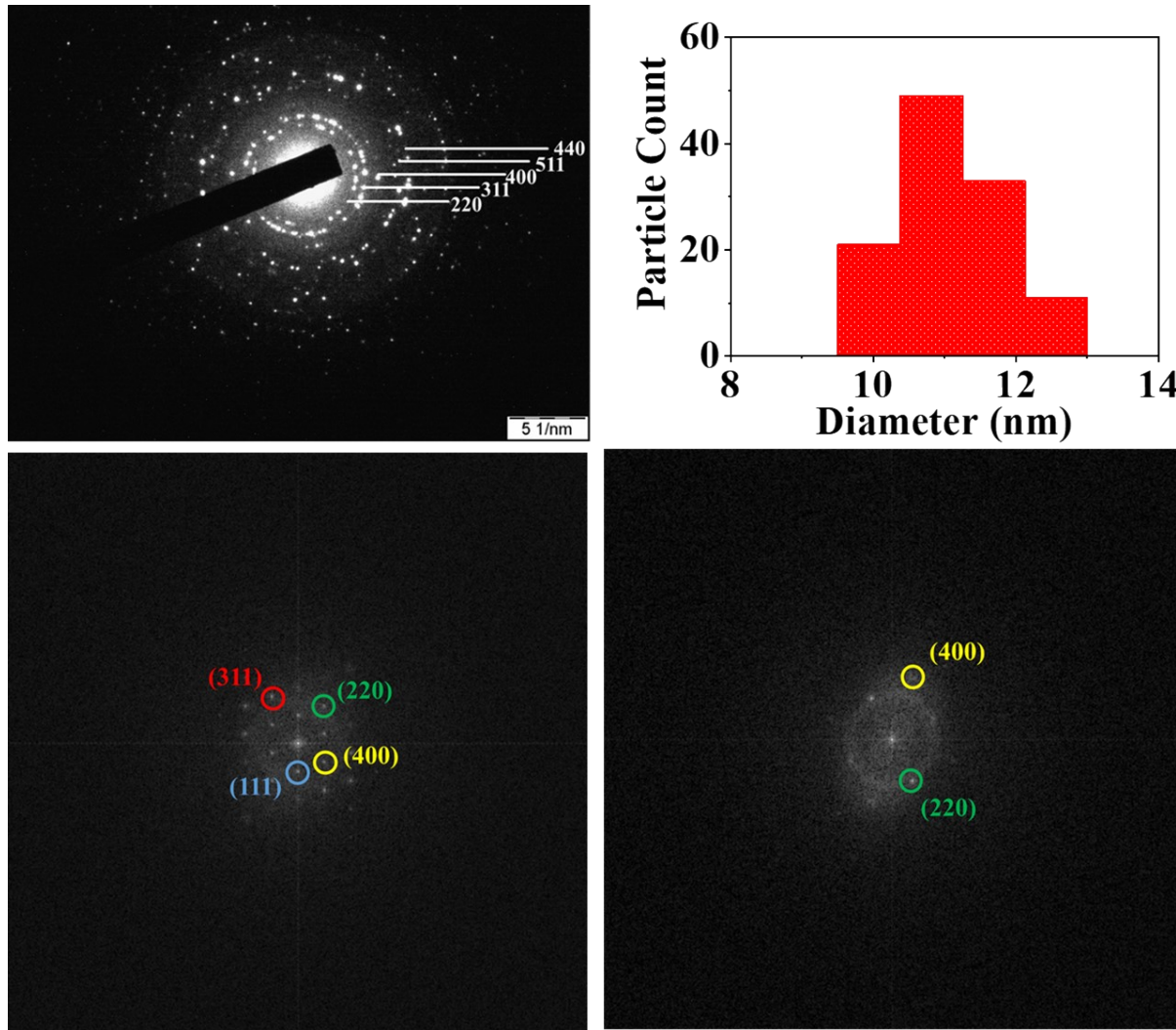


Fig. S3: (a) Indexed SAED patterns for the iron oxide nanospheres; (b) particle size histogram; indexed FFT from (c) dark particle and (d) light particle.

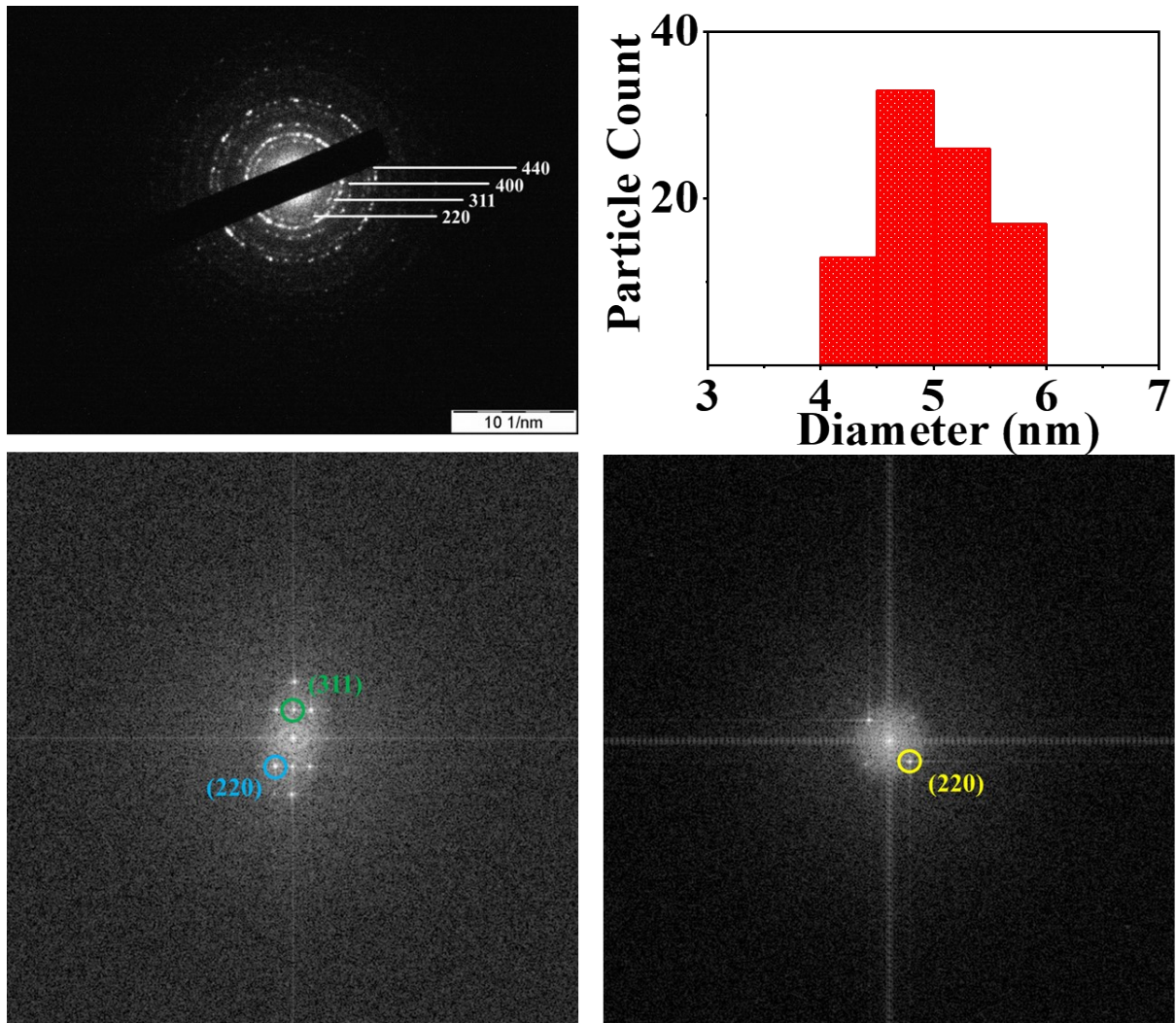


Fig S4: (a) Indexed SAED patterns for the iron oxide nanoparticles in the presence of oleyl alcohol; (b) particle size histogram; indexed FFT from (c) dark particle and (d) light particle.

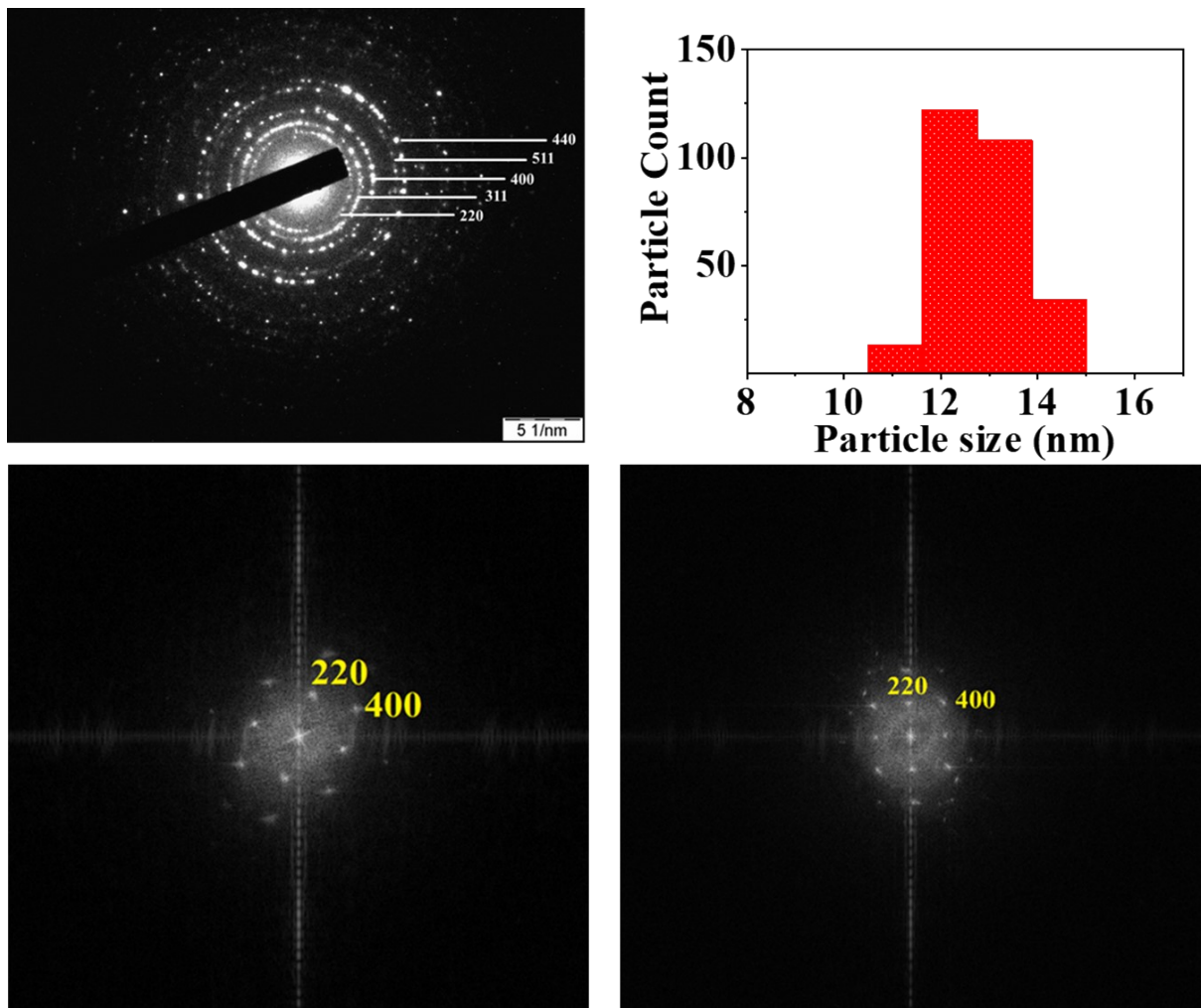


Fig. S5: (a) Indexed SAED patterns for the iron oxide nanocubes; (b) particle size histogram; indexed FFT from (c) light particle and (d) dark particle.

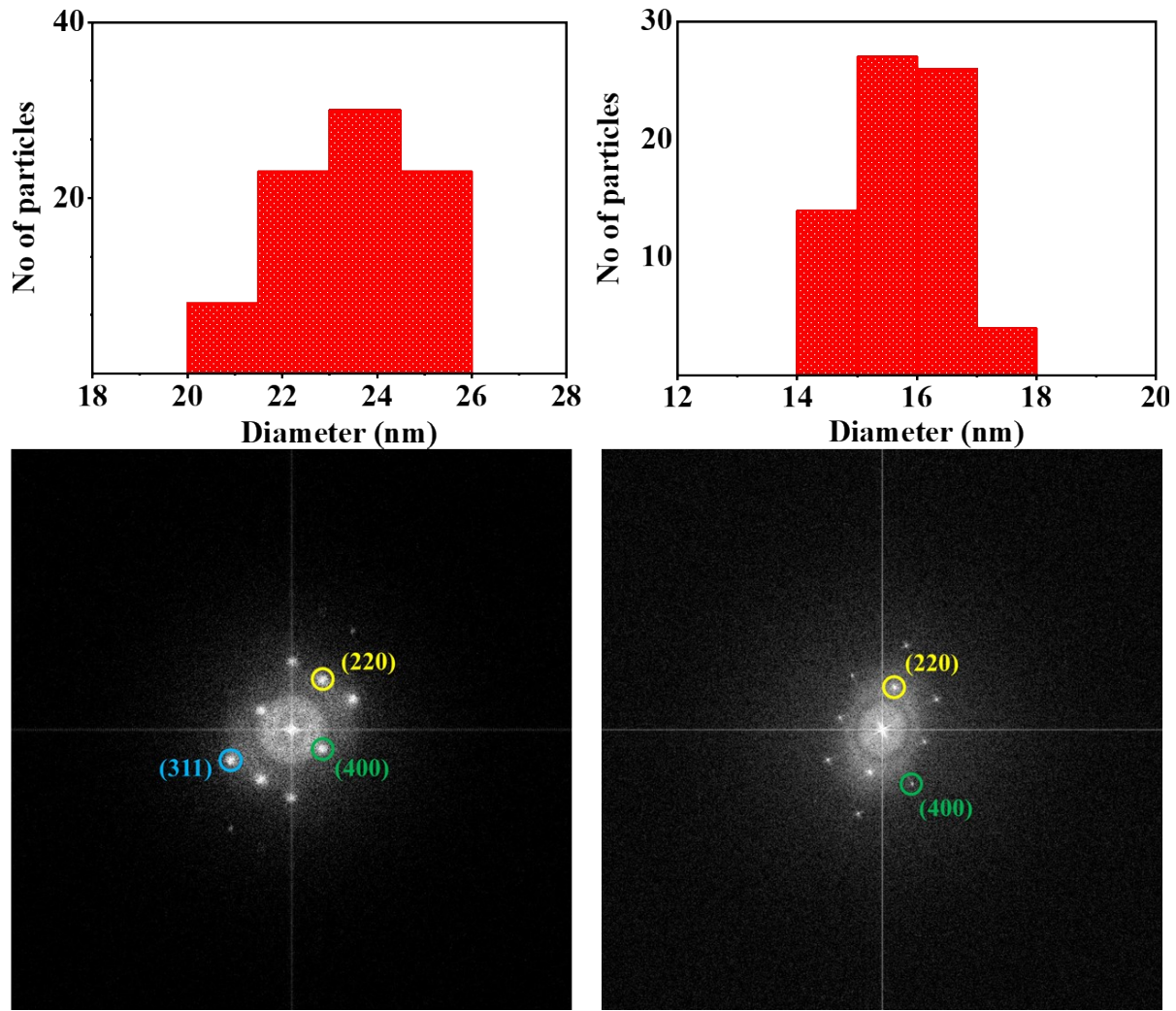


Fig. S6: Particle size histogram of phase-transferred (a) nanospheres and (b) nanocubes; indexed FFT of phase-transferred (c) nanospheres and (d) nanocubes.

Reflux time (hours)	Diameter (nm)
0.5	9 ± 0.75
2	11 ± 0.75
4	14 ± 1
6	19 ± 1

Table S1: Mean Particle size for different reflux times. The temperature was 320°C, and the solvent isobutanol.

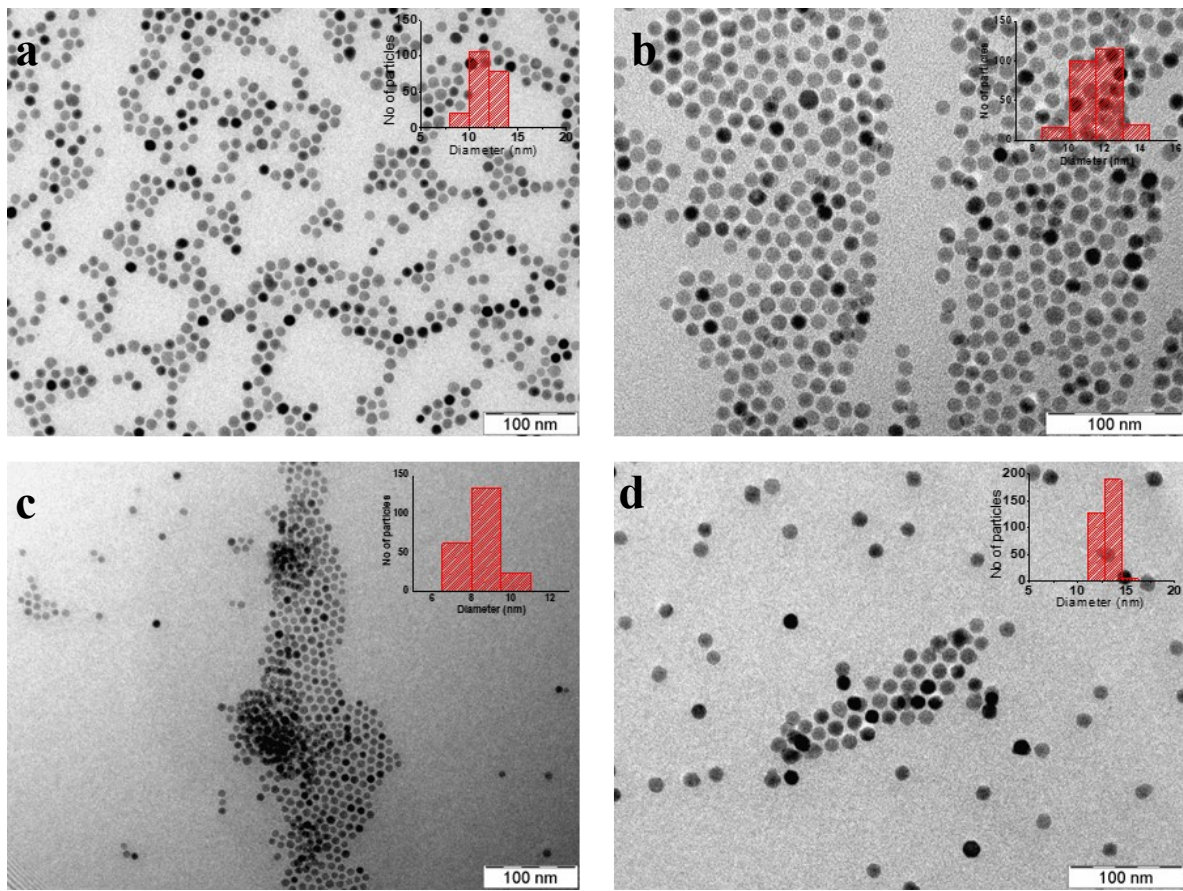


Fig. S7: TEM images of the iron oxide nanoparticles following scheme 1 with methanol (a), ethanol (b), isopropanol (c), and 1-propanol (d) as the starting alcohol.

Alcohol	Diameter (nm)
methanol	11 ± 0.75
ethanol	12 ± 0.75
isopropanol	9 ± 0.5
1-propanol	13 ± 1
Isobutanol	11 ± 0.75

Table S2: Mean particle size for different starting alcohols. The reflux times were 2 hours, and the temperature was 320°C.

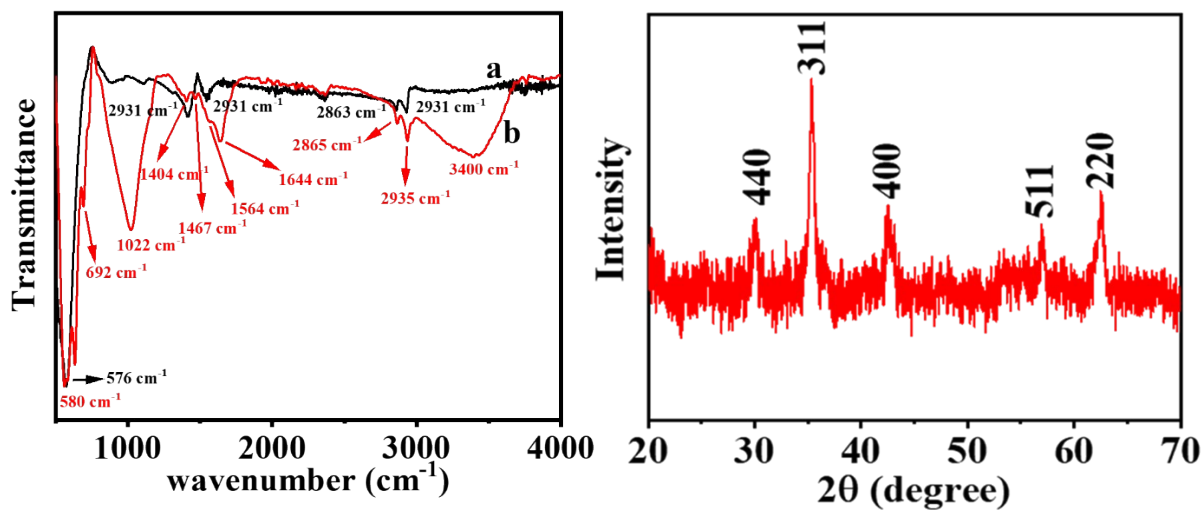


Fig. S8: ATR-IR spectra of oleic acid (a) and NTA-coated iron oxide nanoparticles (b), and the PXRD plot of NTA-capped iron oxide nanoparticles matches with the spinel magneite. The assignment of the IR bands is as follows: oleic acid-capped iron oxide (a): 2931,2863: sp₃ C-H stretching vibration; 1423, 1552: symmetric and asymmetric –COO stretching; 583: Fe-O stretching; NTA-capped iron oxide: 3400: -OH stretching (water); 2935,2865: sp₃ C-H stretching vibration; 1644, 692: N–H bending vibration; 1400: CH₂ scissoring; 1564, 1467: asymmetric and symmetric –COO stretching⁶⁷⁸.

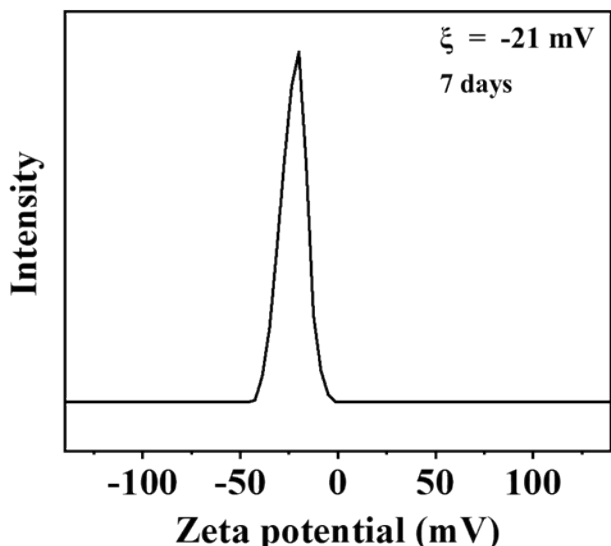
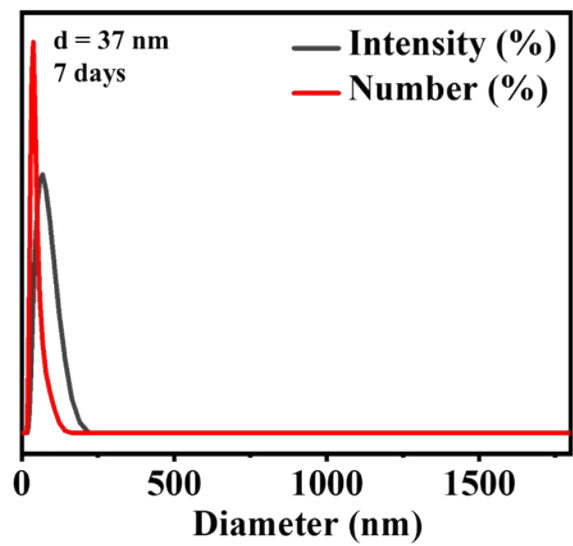
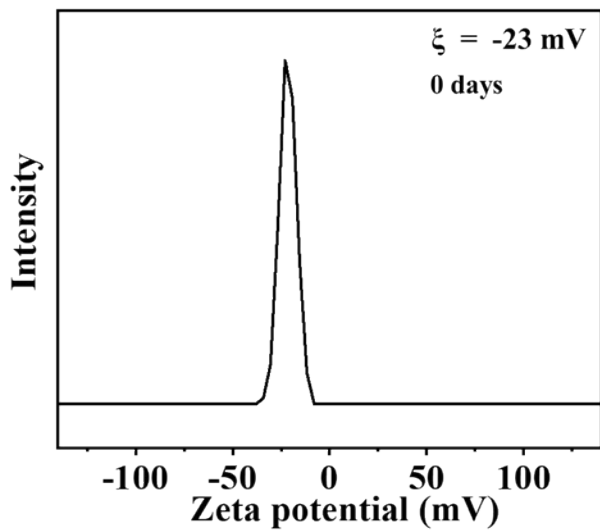
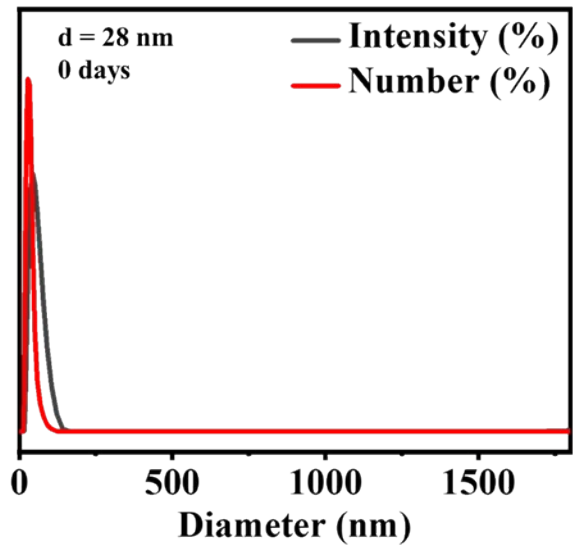


Fig S9: Hydrodynamic particle size measurements (DLS) and zeta potential of the NTA-capped iron oxide nanoparticles immediately after preparation (a and b) and after a gap of seven days (c and d).

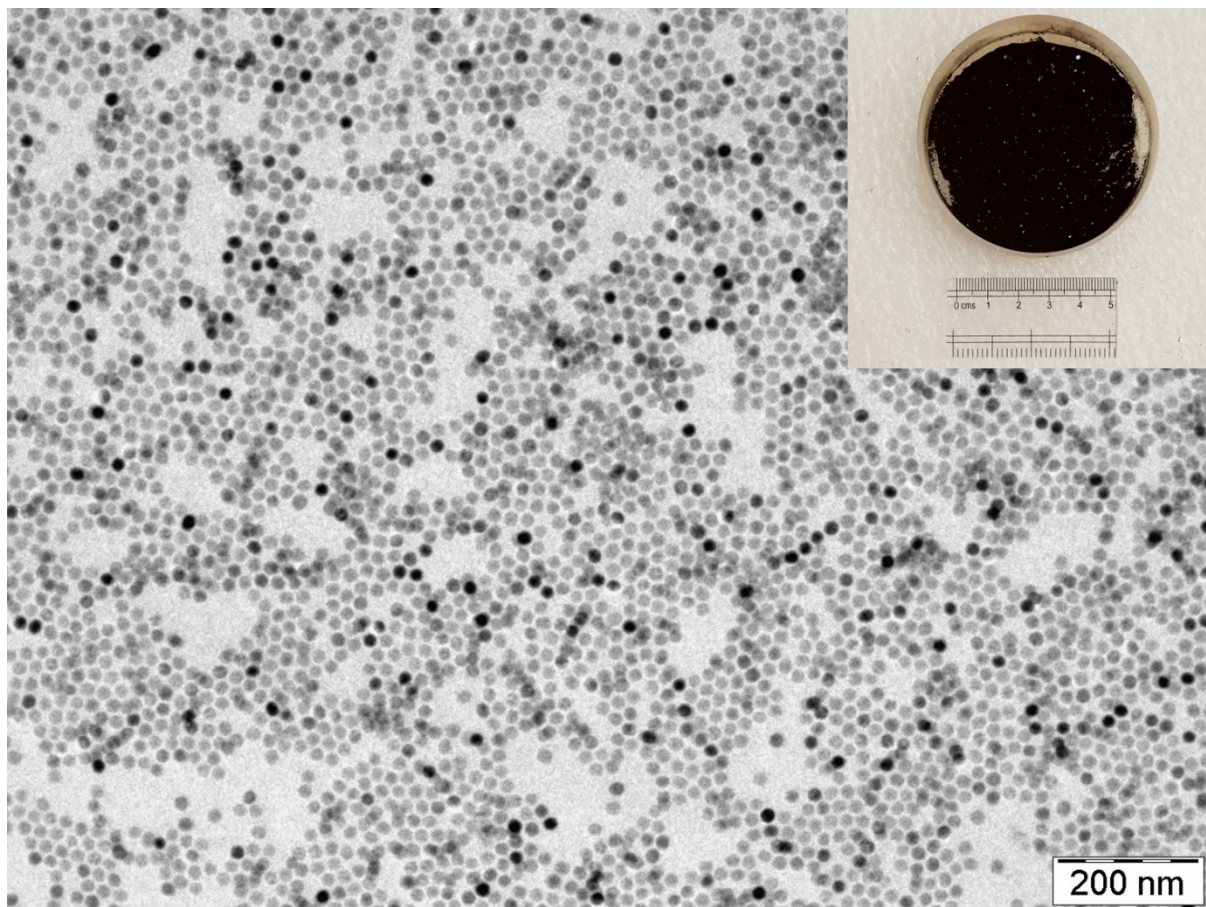


Fig S10: TEM image of single-run gram-scale synthesized monodispersed iron oxide nanoparticles. The inset shows a dried product (5 cm scale for comparison).

References:

- 1 Q. Peng, W. Xu, W. Qi, C. Hu, H. Liu and J. Qu, *Environ. Sci. Pollut. Res.*, 2021, **28**, 63319–63329.
- 2 G. Gunawan, A. Haris, N. B. A. Prasetya, E. Pratista and A. Amrullah, *Indones. J. Chem.*, 2021, **21**, 1397–1407.
- 3 X. Zhao, Y. Su, S. Li, Y. Bi and X. Han, *J. Environ. Sci. (China)*, 2018, **73**, 47–57.
- 4 M. F. B. Stoldt, M. Gonchikzhapov, T. Kasper, U. Fritsching and J. Kiefer, *Phys. Chem. Chem. Phys.*, 2019, **21**, 24793–24801.
- 5 K. S. Sharma, R. S. Ningthoujam, A. K. Dubey, A. Chattopadhyay, S. Phapale, R. R. Juluri, S. Mukherjee, R. Tewari, N. G. Shetake, B. N. Pandey and R. K. Vatsa, *Sci.*

Rep., 2018, **8**, 1–11.

- 6 F. Chen, M. Hong, W. You, C. Li and Y. Yu, *Appl. Surf. Sci.*, 2015, **357**, 856–865.
- 7 Y. Zhou, N. Xu, K. Tian, T. Qing, Y. Hao, P. Liang and M. Li, *Appl. Surf. Sci.*, 2022, **600**, 154102.
- 8 D. Singh, S. Verma, R. K. Gautam and V. Krishna, *J. Environ. Chem. Eng.*, 2016, **3**, 2161–2171.